



Itinerant spin polaron and metallic ferromagnetism in semiconductor moiré superlatticesMargarita Davydova , Yang Zhang ,* and Liang Fu*Department of Physics, Massachusetts Institute of Technology, Cambridge, Massachusetts 02139, USA*

(Received 4 June 2022; revised 3 June 2023; accepted 6 June 2023; published 22 June 2023)

Itinerant spin polaron and metallic ferromagnetism are theoretically predicted in the Mott insulator in semiconductor moiré superlattices doped below and above half filling of the narrow moiré band, respectively. The existence of a spin polaron can be directly identified from the kink in the dependence of the charge gap on the magnetic field.

DOI: [10.1103/PhysRevB.107.224420](https://doi.org/10.1103/PhysRevB.107.224420)

Recent experiments have discovered a plethora of novel electronic phases in transition metal dichalcogenide (TMD) heterostructures, including Mott-Hubbard and charge-transfer insulators [1–6], generalized Wigner crystals [3,7–11], the quantum anomalous Hall state [12], and light-induced ferromagnetism [13]. These remarkably rich phenomena result from strong interaction effects in narrow moiré bands, which generally appear in TMD heterostructures with large moiré wavelengths. Take the example of WSe_2/WS_2 : the lattice corrugation introduced by the moiré structure produces a periodic spatial variation of the valence band edge, which acts as a superlattice potential for charge carriers in the WSe_2 layer. At large moiré wavelength, moiré bands are formed by electron tunneling t between adjacent potential minima, which are well described by a simple tight-binding model on an emergent lattice. The inclusion of the Coulomb interaction between electrons leads to a Hubbard model description. As a hallmark of Hubbard model physics, Mott insulating states are found in angle-aligned WSe_2/WS_2 [3,4] and twisted AB-homobilayer WSe_2 [6] at the filling of $n = 1$ hole per moiré unit cell.

One of the fundamental features of the Hubbard model is the local moment formation driven by the on-site repulsion U . The presence of local moments in WSe_2/WS_2 has been observed by measuring the dependence of optical circular dichroism on the magnetic field [4]. It is found that the exciton Zeeman splitting, which is directly related to the magnetization, saturates above a certain field where the spins are fully polarized. The saturation field depends on the filling factor n and reaches the maximum at $n = 1$, as expected from the Hubbard model.

In this work, we study the charge excitations of the Mott insulator in TMD moiré superlattices in the presence of a magnetic field. By exactly solving the problem of the Mott insulator with one doped hole, we find that as the magnetic field is reduced, the fully polarized state becomes unstable to the formation of a spin polaron—a bound state of a hole

and a spin flip. The spin polaron has a kinetic origin due to the correlated hopping of the hole and the spin flip on the triangular lattice. Importantly, the binding energy of the spin polaron is on the order of the hole hopping amplitude t and has a strong dependence on the center-of-mass momentum \mathbf{P} , which we determine exactly. Our work establishes a spin polaron, a heavy-mass fermion of charge $-e$ and spin $\frac{3}{2}$, as the fundamental charge carrier in a hole-doped Mott insulator over a wide range of magnetic fields, which are experimentally accessible. In contrast, the charge carrier in the electron-doped Mott insulator is the doublon with charge e and spin of $\frac{1}{2}$.

The dichotomy between the charge excitations of opposite signs leads to distinct phases that arise upon doping below and above $n = 1$. At $n = 1 + \delta$ ($\delta > 0$), metallic (Nagaoka) ferromagnetism is favored by the kinetic motion of doublons. At $n = 1 - \delta$, a strange metallic state is formed by the dilute Fermi gas of spin polarons with incomplete spin polarization and a gap to adding or removing a charge carrier. As a direct manifestation of the electron-hole asymmetry, we predict a discontinuous jump of the saturation field across $n = 1$. We further propose compressibility measurements for detecting spin polarons in TMD moiré materials directly. Our work reveals doping-induced itinerant magnetic states in semiconductor moiré systems, whose energy scale is defined by the kinetic energy much larger than the exchange interactions.

The early work [14] identified spin polaron in the context of superconductivity in an extended Hubbard model on the triangular lattice. Related physics in the context of ultracold atoms has been studied using a t - J model [15]. Compared to these studies, our work not only introduces TMD moiré superlattices as the promising material platform for the realization of spin polaron, but also identifies its experimental manifestation, namely, the dependence of the charge gap on the magnetic field.

I. HUBBARD MODEL DESCRIPTION AND THE MOTT INSULATOR AT $n = 1$

The starting point for our analysis of a TMD moiré heterobilayer under a magnetic field is the canonical Hubbard model

*Present address: Department of Physics and Astronomy, University of Tennessee, Knoxville, Tennessee 37996, USA; Min H. Kao Department of Electrical Engineering and Computer Science, University of Tennessee, Knoxville, Tennessee 37996, USA.

on a triangular lattice [1]:

$$H = -t \sum_{\langle i,j \rangle} (c_i^\dagger c_j + \text{H.c.}) + U \sum_i n_{i\uparrow} n_{i\downarrow} + \frac{h}{2} \sum_i (n_{i\uparrow} - n_{i\downarrow}). \quad (1)$$

c_i^\dagger is the creation operator of a doped charge in the moiré superlattice. For simplicity of presentation, we assume the doped charge is of electron type. As we discuss later, the long-range Coulomb interaction does not affect the formation of a spin polaron in the limit of large Hubbard U . For typical TMD moiré materials, $t \sim 1$ meV [2] is much smaller than the on-site Coulomb repulsion U , leading to the strong-coupling regime of the Hubbard model.

At half-filling ($n = 1$), the Mott insulator is a quantum antiferromagnet governed by the spin- $\frac{1}{2}$ Heisenberg model on the triangular lattice: $H_J = J \sum_{\langle ij \rangle} \mathbf{s}_i \cdot \mathbf{s}_j$, with $J = 4t^2/U$ and \mathbf{s} is the spin- $\frac{1}{2}$ operator. Since $t \ll U$, the antiferromagnetic exchange interaction J in TMD moiré superlattices is generally weak [16]. As a result, the antiferromagnetic Mott insulator becomes fully polarized above a small saturation field h_s^0 whose value is set by J [see the Supplemental Material (SM) [24]]: $h_s^0 = \frac{9}{2}J = 18\frac{t^2}{U}$, where the superscript “0” refers to an undoped Mott insulator. For example, using $t = 1$ meV and assuming $U \sim 50$ meV for angle-aligned WSe₂/WS₂, J is only 0.08 meV and the corresponding saturation field is 1 T (using the g factor 6.7 for holes in WSe₂). This value is comparable to the saturation field measured by magnetic circular dichroism at $n = 1$ [4].

Thanks to the narrow bandwidth, the full magnetization curve of TMD moiré materials can be measured over the entire range of filling factors $0 \leq n \leq 2$, which is not possible elsewhere. The ability to achieve full spin polarization in doped Mott insulators opens access to rich and previously unexplored Hubbard model physics on the triangular lattice, as we shall show below.

II. CHARGE EXCITATIONS IN MOTT INSULATOR

As a first step towards the study of doped Mott insulators, we consider charge excitations of the Mott insulator at $n = 1$ at full spin polarization induced by a magnetic field $h > h_s^0$. Interestingly, we find that the charge e and $-e$ excitations have very different nature, as represented in Fig. 1.

Charge e excitation is simply a doublon created by adding an electron with minority spin, which costs a minimum energy

$$E_d = E_d^0 + \frac{h}{2} = U - \mu - 6t + \frac{h}{2}, \quad (2)$$

where E_d^0 is the minimum energy of the doublon in the absence of magnetic field, μ is the chemical potential, $-6t$ comes from the kinetic energy of the added electron at the bottom of the band at $\mathbf{k} = 0$, and $h/2$ comes from the Zeeman energy of the added minority spin. The nature of charge $-e$ excitation depends on the magnetic field h . When h is sufficiently large, the lowest-energy excitation is simply a hole

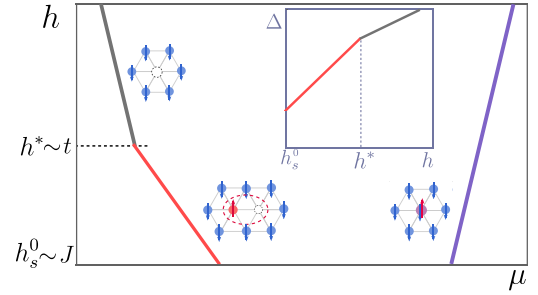


FIG. 1. The gap edges of the Mott insulator as a function of the magnetic field h . The upper and lower edges of the gap are defined by the energy cost of adding a charge e and $-e$ quasiparticle, respectively. The charge e quasiparticle is a $s = \frac{1}{2}$ doublon. The charge $-e$ quasiparticle transitions from a $s = \frac{1}{2}$ hole to a $s = \frac{3}{2}$ spin polaron at $h = h^* = \varepsilon_b - E_{sw}^0 \sim t$, resulting in a change of slope in the lower gap edge and the charge gap at $n = 1$ (inset).

with a minimum energy given by

$$E_h = E_h^0 + \frac{h}{2} = \mu - 3t + \frac{h}{2}, \quad (3)$$

where $E_h^0 = \mu - 3t$ is the minimum energy of the hole in the absence of magnetic field, which comes from the kinetic energy of the hole at the band maxima $\mathbf{k} = \pm\mathbf{K}$.

However, when the magnetic field is reduced below a certain value h^* (with $h^* \gg h_s^0$ for $t \gg J$; we assume well-separated scales of energies here for clarity, and address more realistic parameters later on), we find that the lowest energy state of the Mott insulator with one hole is no longer fully spin polarized, but contains one spin flip that is bound to a hole. The bound state of the hole and the spin flip is a spin polaron, a composite quasiparticle carrying spin $s = \frac{3}{2}$ along the field direction. h^* is the saturation field for the Mott insulator with one hole. Viewed from a complementary perspective, h^* is the dividing line between the domains with two types of charge $-e$ excitations in the Mott insulator: the bare hole and the spin polaron.

As we show below, the origin of the spin polaron formation is purely kinetic. The spin flip gains kinetic energy of the order of $t \gg J$ by exchanging its position with an adjacent hole. Remarkably, this highly restricted kinetic process is sufficient to bind them together on the triangular lattice, but not on square or honeycomb lattices. The result is an *itinerant* spin polaron whose binding energy depends on its center-of-mass momentum \mathbf{P} . We find that at $h < h^*$, the energy cost of adding a carrier with charge $-e$ is

$$E_{sp} = E_h + E_{sw} - \varepsilon_b = E_h^0 + E_{sw}^0 + \frac{3h}{2} - \varepsilon_b, \quad (4)$$

where E_{sw}^0 is the minimum kinetic energy of spin waves in the absence of magnetic field and $\varepsilon_b \sim t$ is the binding energy of the spin polaron at zero momentum $\mathbf{P} = 0$. The total Zeeman energy $\frac{3h}{2}$ comes from the $s = \frac{3}{2}$ of the spin polaron.

Comparing the expressions for E_{sp} and E_h , we see that the spin polaron has lower energy than a hole at $h < h^*$ with $h^* = \varepsilon_b - E_{sw}^0$. At large Hubbard U , the binding energy $\varepsilon_b \sim t$ is significantly larger than $E_{sw}^0 \sim J = 4\frac{4t^2}{U}$. In a wide range of fields $h_s^0 \sim J < h < h^* \sim t$, spin polarons are the lowest-

energy charge carriers upon hole doping of the Mott insulator. Note that our spin polaron exists on top of the field-polarized state of the Mott insulator, which is fundamentally different from the magnetic polaron in quantum antiferromagnets at $h = 0$ [17–22]. For example, since the noncollinear antiferromagnetic state on the triangular lattice spontaneously breaks spin rotational symmetry, the magnetic polaron at $h = 0$ does not have a well-defined spin quantum number, in contrast with the $s = \frac{3}{2}$ spin polaron we find here.

The field-induced transition in the type of the charged excitations is reflected in the charge gap of the Mott insulator, defined as $\Delta = E_{+e} + E_{-e}$:

$$\Delta(h) = \begin{cases} \Delta_0 + h, & h > h^*, \\ \Delta_0 + E_{sw}^0 - \varepsilon_b + 2h, & h_s^0 < h < h^*, \end{cases} \quad (5)$$

where Δ_0 is field independent. Due to the different spin quantum numbers of the hole and the spin polaron, $\Delta(h)$ shows a change of slope at h^* , as illustrated in Fig. 1.

Remarkably, because of its purely kinetic origin, the spin polaron appears already in the limit $U = \infty$ ([14]; see also [15,23]). In what follows, we start by considering $U = \infty$ first ($t/U = 0$). Next, we study the spin polaron formation and the saturation field at finite t/U , showing that surprisingly, the binding between the hole and the spin flip is further *enhanced* at finite t/U . We finally conclude by discussing experimental signatures of the spin polaron.

III. SPIN POLARON

Let us first study the spin polaron in the limit $U \rightarrow \infty$, where the physical picture becomes especially simple. A single hole or doublon with momentum \mathbf{k} will have energy $\varepsilon_{h/d}(\mathbf{k}) = \frac{h}{2} \pm t\gamma_{\mathbf{k}}$ with $\gamma_{\mathbf{k}} = \sum_n (e^{ik \cdot \mathbf{t}_n} + e^{-ik \cdot \mathbf{t}_n})$, where $\mathbf{t}_{n=1,2,3}$ are the three basis vectors on a triangular lattice. We examine the state containing one hole and one spin flip using the general ansatz:

$$|\psi_h\rangle = \sum_{n,m} \alpha_{nm} c_{n\downarrow} S_m^+ |FM_{n=1}\rangle. \quad (6)$$

Here, $S_m^+ \equiv c_{m\uparrow}^\dagger c_{m\downarrow}$. The vacuum state corresponds to a fully polarized state with single occupancy at each site $|FM_{n=1}\rangle = \prod_i c_{i\downarrow}^\dagger |0\rangle$. The wave function must necessarily vanish at the origin, reflecting the fact that the positions of a spin flip and a hole cannot coincide.

The Hubbard Hamiltonian at $U = \infty$, which forbids double occupancy, acting on Eq. (6) reduces to a two-particle problem. This problem can be separated into center of mass and relative motion, which in relative coordinates becomes a version of a tight-binding model on a triangular lattice. The details of the calculation are provided in the Supplemental Material [24]. We find that at $\mathbf{P} = 0$, the bound state of a hole and a spin flip occurs for one of the inversion-odd representations of the group D_6 and follows from the especially simple self-consistency equation

$$1 + \sum_q \frac{2t \sin \mathbf{q} \cdot \mathbf{t}_1 (\sin \mathbf{q} \cdot \mathbf{t}_1 + \sin \mathbf{q} \cdot \mathbf{t}_2 + \sin \mathbf{q} \cdot \mathbf{t}_3)}{E - \frac{3}{2}h - t\gamma_{\mathbf{q}}} = 0. \quad (7)$$

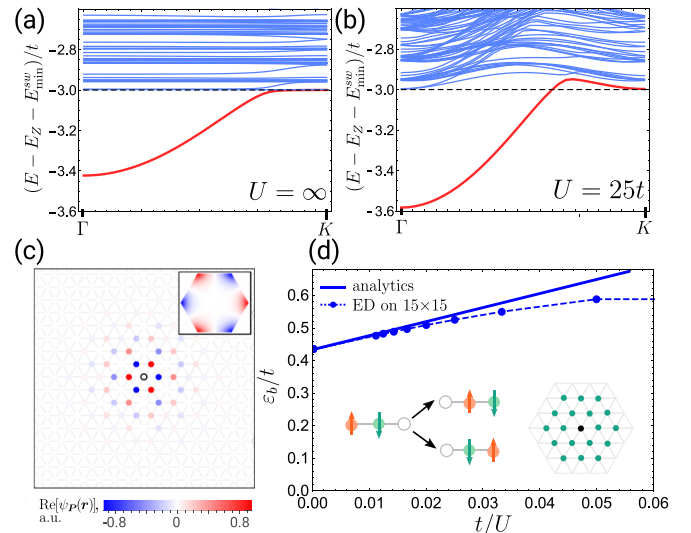


FIG. 2. The energy spectrum of the Hubbard model at $n = 1$ doped with one hole as a function of the center-of-mass momentum \mathbf{P} along the Γ - K direction at (a) infinite U and (b) $U = 25t$. The dispersive bound state (red line) is found below the continuum spectrum (blue); the total Zeeman energy of the state and the minimum energy of spin waves are $E_Z = \frac{3}{2}h$ and $E_{sw}^{\min} = 18 \frac{t^2}{U} = \frac{9}{2}J$. (c) The real-space wave function in relative coordinates for $\mathbf{P} = \mathbf{0}$ at $U = \infty$. Inset: momentum-space wave function in relative coordinates. (d) The binding energy of the spin polaron increases as a function of t/U . The results of the exact diagonalization of the full Hubbard model on a 15×15 lattice and of the analytical approach at order t^2/U are shown by dots and a solid line, correspondingly.

This produces a bound state (spin polaron) with energy $E_{sp}(\mathbf{P} = 0) = E_h - \varepsilon_b^{(0)} + h$, where the binding energy is found to be $\varepsilon_b^{(0)} \equiv \varepsilon_b(\mathbf{P} = 0) \approx 0.42t$ and the $+h$ contribution is the energetic cost of a spin flip. The fact that the binding energy is proportional to t indicates the kinetic origin of spin polaron formation as we discussed above.

Next, we solve the tight-binding equation describing the relative motion of the hole and the spin flip with a finite center-of-mass momentum in order to find the spin polaron dispersion. The spectrum for \mathbf{P} along the Γ - K direction obtained from exact diagonalization of the tight-binding equation on a lattice of 866 sites with periodic boundary conditions is shown in Fig. 2(a). The dispersive bound state is found below the band bottom. We find that the mass of the bound state is $m_{sp} \approx 13m_h$, where the mass of the bare hole is $m_h = \frac{2}{3} \frac{1}{ta^2}$. Figure 2(c) shows the real-space wave function of the spin polaron in the relative coordinates at $\mathbf{P} = 0$. The spin polaron is tightly bound on a length scale of the order of one lattice spacing and the wave function realizes the one-dimensional antisymmetric irrep Γ_3 of the dihedral group D_6 and vanishes exactly at the origin. As seen in Fig. 2(a), the state merges with continuum at $\mathbf{P} = K$.

For a single doublon, we find, both analytically using the approach described above and numerically (see SM), that the spin polaron does not form. It similarly does not form on the square lattice, for either doping. In particular, this is dictated by the symmetry of the solution: the wave function of the bound states must vanish at the origin in the

relative coordinates, i.e., $\alpha_{mn} = \beta_{mn} = 0$. The single-particle spectrum of a doped electron on the triangular lattice, or doped electron/hole on a square lattice has only one band minimum and therefore, the low-energy states of such excitations cannot have a node. In contrast, on the triangular lattice, the hole dispersion has two band minima at $\pm K$ points. An antisymmetric superposition of $\pm K$ states, shown in the inset in Fig. 2(b), allows for the existence of a spin polaron.

In the case of the charge-transfer insulator described by multi-band Hubbard models [2,25], the dispersion of the charge carriers doped below the fully polarized state at $n = 1$ still has two band minima at $\pm K$, which leads to the spin polaron formation. The situation will be different for electron doping, which we leave to a future study.

IV. FINITE U

We now consider the effect of large finite U (small nonzero t/U). The effective Hamiltonian at the order t^2/U includes not only the spin exchange, but also the correlated hopping. The correlated hopping comes from the second-order processes wherein the spin or the hole can move over one or two sites [see the inset in Fig. 2(d)]. Importantly, these processes only occur when the hole and the spin flip are in the vicinity of each other. While the correlated hopping is commonly ignored in the literature [15,23], we show that these microscopic kinetic processes can have important effects on spin polaron formation.

We obtain the full analytical solution for the bound state problem at the order $\frac{t^2}{U}$ (see SM). The spectrum of the spin polaron is shown in Fig. 2(b) at $U = 25t$. In Fig. 2(d), we plot the dependence of the binding energy on t/U as obtained from the analytical approach at the order $\frac{t^2}{U}$. Also shown is the result of the exact diagonalization of the full Hubbard model Hamiltonian on a 15×15 lattice in the appropriate spin and charge sectors. The two methods show excellent agreement up to $t/U \approx 0.05$, which corresponds to $J/t \approx 0.2$. Remarkably, the binding energy of the spin polaron *increases* with t/U . At large but finite U , the spin flip can become delocalized to lower its kinetic energy, which competes with the formation of the bound state. Nevertheless, the proximity to the hole enables a large number of correlated hopping processes on the triangular lattice, which leads to an additional gain in kinetic energy. This increases the binding energy of the spin polaron and dominates over the spin delocalization. Thus, correlated hopping enhances the stability of spin polarons at finite U , an effect which has been overlooked before [14]. In contrast, neglecting correlated hopping, i.e., working with the t - J model, will produce a decrease in the binding energy with t/U (see Fig. S8 in the SM), which is incorrect.

V. FINITE DOPING

We now consider the case of finite doping density. The Hubbard model on triangular lattice has been extensively studied in the absence of magnetic field. It is known that, at $U \gg t$ and for the electron doping ($n > 1$), the Nagaoka ferromagnetic state [26–28] arises due to the kinetic

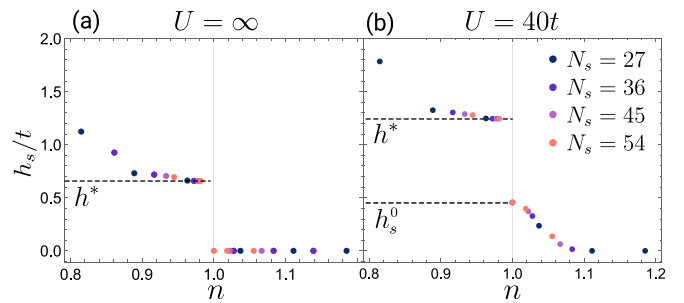


FIG. 3. The saturation field h_s at different fillings obtained by exact diagonalization of the Hubbard model with an odd number of doped electrons/holes on $3 \times L$ geometry with $L = 9, 12, 15, 18$ in the sector with a single spin flip. Panel (a) represents the limit $U = \infty$ and panel (b) corresponds to $U = 40t$. The dashed black line shows the field h^* for the undoped Mott insulator at $n = 1$.

energy gain of the doublons, which dominates over the weaker antiferromagnetic exchange interaction between localized spins $J = 4t^2/U \ll t$. In contrast, for any amount of doped holes, the ferromagnetic state is unstable at zero magnetic field [27–31], while the nature of the true ground state is hard to determine.

Our results provide insight on charge excitations of the Mott insulator under a magnetic field. As we have shown, while the undoped Mott insulator is already fully polarized at small magnetic fields above $h_s^0 \sim J \propto t^2/U$, the state with one hole can only achieve full polarization above a larger field $h^* \sim t > h_s^0$, at which the first spin flip appears that is bound to the hole. Now consider a finite but small density δ of holes. At high field, the fully polarized state is a dilute Fermi gas of holes. As the field is reduced, provided that the hole density is sufficiently low, the first spin flip to appear should also bind with one hole. It follows from this argument that the saturation field h_s at finite hole density should approach h^* as $\delta \rightarrow 0$. In contrast, upon electron doping, the Nagaoka mechanism eventually leads to a ferromagnetic ground state at zero external field (or immediately becomes ferromagnetic in the limit $U = \infty$). Note that h^* remains finite even when $U = \infty$, whereas $h_s^0 = 0$ in this limit. Therefore, we conclude that the saturation field as a function of doping shows a *discontinuous* jump from $h_s = h^*$ at $n = 1^-$ to $h_s^0 < h^*$ at $n = 1^+$.

This conclusion is supported by our calculation of the saturation field h_s as a function of doping, using exact diagonalization of the Hubbard model shown in Fig. 3. The calculations were performed at a fixed number of holes $N_h = 1, 3, 5$ on three-leg ladders with periodic boundary conditions and various lengths $L = 9, 12, 15, 18$. By comparing the energy of the state with a single spin flip to that of a fully polarized state, we obtain a lower bound on the saturation field. Figure 3 shows the results of exact diagonalization for the infinite- U Hubbard model and at $U = 40t$. On the hole-doping side, the field h_s approaches h^* (its value is enhanced because of the finite-width effects, and fully agrees with our tight-binding calculation). The parameters that we chose are realistic for many TMD moiré materials [2], where a large window of magnetic fields exists for the spin polaron predicted here to be observed. On the electron-doping side the saturation field equals h_s^0 at $n \rightarrow 1^+$ and exhibits behavior

expected from a Nagaoka ferromagnet at infinite and finite Hubbard U , as seen in panels (a) and (b).

Finally, we discuss the effect of the long-range Coulomb repulsion $\sum V_{ij}n_i n_j$ on the binding energy of spin polarons. At $U = \infty$, it does not affect the energy of a single-spin polaron, because the system contains only one hole and its Coulomb energy is independent of the spin configuration. At finite but large U there will be a small correction of the order of $\frac{t^2 V}{U} \ll t$ due to the small amplitude of admixing doublons.

VI. EXPERIMENTAL IMPLICATIONS

The particle-hole asymmetry of the saturation field, especially its discontinuity at $n = 1$, reflects the distinction between the doublon and the spin polaron in the doped Mott insulator on the triangular lattice. In light of our theory, it is encouraging to note that the saturation field in WSe_2/WS_2 measured at $T = 1.7$ K [4] indeed decreases with doping at $n > 1$, increases with doping at $n < 1$, and shows a large rapid change across $n = 1$, which we expect will sharpen into a discontinuity at $T = 0$.

The presence of a spin polaron can be established by the dependence of the lower edge of the Mott gap at $n = 1$ on the

magnetic field, which can be obtained from compressibility measurements. As shown in Fig. 1, our theory predicts a linear dependence of the lower gap edge on the field with a change in the slope by a factor of 3 at $h = h^*$, which shows the different spin quantum numbers: $s = \frac{3}{2}$ for the spin polaron and $s = \frac{1}{2}$ for the bare charge carrier below $n = 1$.

Our theory predicts that at small hole doping, a Fermi liquid of $s = \frac{3}{2}$ spin polarons can form in a range of magnetic fields below h^* and above h_s^0 . This is a pseudogap metallic state with heavy fermion mass that has a gap to adding an $s = \frac{1}{2}$ electron/hole, and also exhibits filling-dependent magnetization plateaus. Its detailed study appeared in Ref. [32].

Note added. Recently, measurements of electronic compressibility in twisted double bilayer WSe_2 [33] revealed a kink in the charge gap as a function of magnetic field, consistent with our theory of the transition between the spin polaron and the bare hole quasiparticles.

ACKNOWLEDGMENTS

This work was supported by the Air Force Office of Scientific Research (AFOSR) under award FA9550-22-1-0432 and the David and Lucile Packard Foundation.

-
- [1] F. Wu, T. Lovorn, E. Tutuc, and A. H. MacDonald, *Phys. Rev. Lett.* **121**, 026402 (2018).
 - [2] Y. Zhang, N. F. Q. Yuan, and L. Fu, *Phys. Rev. B* **102**, 201115(R) (2020).
 - [3] E. C. Regan, D. Wang, C. Jin, M. I. Bakti Utama, B. Gao, X. Wei, S. Zhao, W. Zhao, Z. Zhang, K. Yumigeta *et al.*, *Nature (London)* **579**, 359 (2020).
 - [4] Y. Tang, L. Li, T. Li, Y. Xu, S. Liu, K. Barmak, K. Watanabe, T. Taniguchi, A. H. MacDonald, J. Shan *et al.*, *Nature (London)* **579**, 353 (2020).
 - [5] T. Li, S. Jiang, L. Li, Y. Zhang, K. Kang, J. Zhu, K. Watanabe, T. Taniguchi, D. Chowdhury, L. Fu *et al.*, *Nature (London)* **597**, 350 (2021).
 - [6] Y. Xu, K. Kang, K. Watanabe, T. Taniguchi, K. F. Mak, and J. Shan, *Nat. Nanotech* **17**, 934 (2022).
 - [7] Y. Xu, S. Liu, D. A. Rhodes, K. Watanabe, T. Taniguchi, J. Hone, V. Elser, K. F. Mak, and J. Shan, *Nature (London)* **587**, 214 (2020).
 - [8] Y. Zhou, J. Sung, E. Brutschea, I. Esterlis, Y. Wang, G. Scuri, R. J. Gelly, H. Heo, T. Taniguchi, K. Watanabe *et al.*, *Nature (London)* **595**, 48 (2021).
 - [9] C. Jin, Z. Tao, T. Li, Y. Xu, Y. Tang, J. Zhu, S. Liu, K. Watanabe, T. Taniguchi, J. C. Hone *et al.*, *Nat. Mater.* **20**, 940 (2021).
 - [10] H. Li, S. Li, E. C. Regan, D. Wang, W. Zhao, S. Kahn, K. Yumigeta, M. Blei, T. Taniguchi, K. Watanabe *et al.*, *Nature (London)* **597**, 650 (2021).
 - [11] X. Huang, T. Wang, S. Miao, C. Wang, Z. Li, Z. Lian, T. Taniguchi, K. Watanabe, S. Okamoto, D. Xiao *et al.*, *Nat. Phys.* **17**, 715 (2021).
 - [12] T. Li, S. Jiang, B. Shen, Y. Zhang, L. Li, Z. Tao, T. Devakul, K. Watanabe, T. Taniguchi, L. Fu *et al.*, *Nature (London)* **600**, 641 (2021).
 - [13] X. Wang, C. Xiao, H. Park, J. Zhu, C. Wang, T. Taniguchi, K. Watanabe, J. Yan, D. Xiao, D. R. Gamelin *et al.*, *Nature (London)* **604**, 468 (2022).
 - [14] S.-S. Zhang, W. Zhu, and C. D. Batista, *Phys. Rev. B* **97**, 140507(R) (2018).
 - [15] I. Morera, A. Bohrdt, W. W. Ho, and E. Demler, *arXiv:2106.09600*.
 - [16] N. C. Hu and A. H. MacDonald, *Phys. Rev. B* **104**, 214403 (2021).
 - [17] C. L. Kane, P. A. Lee, and N. Read, *Phys. Rev. B* **39**, 6880 (1989).
 - [18] P. A. Lee, N. Nagaosa, and X.-G. Wen, *Rev. Mod. Phys.* **78**, 17 (2006).
 - [19] S. Sachdev, *Phys. Rev. B* **39**, 12232 (1989).
 - [20] S. Schmitt-Rink, C. M. Varma, and A. E. Ruckenstein, *Phys. Rev. Lett.* **60**, 2793 (1988).
 - [21] W. P. Su and X. Y. Chen, *Phys. Rev. B* **38**, 8879 (1988).
 - [22] J. R. Schrieffer, X.-G. Wen, and S.-C. Zhang, *Phys. Rev. Lett.* **60**, 944 (1988).
 - [23] I. Morera, M. Kanász-Nagy, T. Smolenski, L. Ciorciaro, A. Imamoğlu, and E. Demler, *Phys. Rev. Res.* **5**, L022048 (2023).
 - [24] See Supplemental Material at <http://link.aps.org/supplemental/10.1103/PhysRevB.107.224420> for the full details on the derivations, and comparison to the t - J model predictions.
 - [25] Y. Zhang, T. Liu, and L. Fu, *Phys. Rev. B* **103**, 155142 (2021).
 - [26] Y. Nagaoka, *Phys. Rev.* **147**, 392 (1966).
 - [27] T. Hanisch, B. Kleine, A. Ritzl, and E. Müller-Hartmann, *Ann. Phys.* **507**, 303 (1995).
 - [28] B. S. Shastry, H. R. Krishnamurthy, and P. W. Anderson, *Phys. Rev. B* **41**, 2375 (1990).
 - [29] H. Tasaki, *Phys. Rev. B* **40**, 9192 (1989).
 - [30] P. Richmond and G. Rickayzen, *J. Phys. C* **2**, 528 (1969).
 - [31] J. O. Haerter and B. S. Shastry, *Phys. Rev. Lett.* **95**, 087202 (2005).
 - [32] Y. Zhang and L. Fu, *SciPost Phys. Core* **6**, 038 (2023).
 - [33] B. A. Foutty, J. Yu, T. Devakul, C. R. Kometter, Y. Zhang, K. Watanabe, T. Taniguchi, L. Fu, and B. E. Feldman, *Nat. Mater.* **22**, 731 (2023).